



Knowledge-based planning using pseudo-structures for volumetric modulated arc therapy (VMAT) of postoperative uterine cervical cancer: a multi-institutional study

Tatsuya Kamima¹, Yoshihiro Ueda², Jun-ichi Fukunaga³, Mikoto Tamura⁴, Yumiko Shimizu⁵, Yuta Muraki⁵, Yasuo Yoshioka¹, Nozomi Kitamura¹, Yuya Nitta², Masakazu Otsuka⁴, Hajime Monzen⁴

¹Radiation Oncology Department, Cancer Institute Hospital, Japanese Foundation for Cancer Research, Tokyo, Japan

²Department of Radiation Oncology, Osaka International Cancer Institute, Osaka, Japan

³Division of Radiology, Department of Medical Technology, Kyushu University Hospital, Fukuoka, Japan

⁴Department of Medical Physics, Graduate School of Medical Sciences, Kindai University, Osaka, Japan

⁵Department of Radiology, Seirei Hamamatsu General Hospital, Shizuoka, Japan

ABSTRACT

Background: The aim of this study was to investigate the performance of the RapidPlan (RP) using models registered pseudo-structures, and to determine how many structures are required for automatic optimization of volumetric modulated arc therapy (VMAT) for postoperative uterine cervical cancer.

Materials and methods: Pseudo-structures around the PTV were retrospectively contoured for patients who had completed treatment at five institutions. For 22 common patients, plans were generated with a single optimization for models with two (RP_2), four (RP_4), and five (RP_5) registered structures, and the dosimetric parameters of these models were compared with a clinical plan with several optimizations.

Results: Most dosimetric parameters showed no major differences between each RP model. In particular, the rectum D_{max} , V_{50Gy} , and V_{40Gy} with RP_2, RP_4, and RP_5 were not significantly different, and were lower than those of the clinical plan. The average proportions of plans achieving acceptable criteria for dosimetric parameters were close to 100% for all models. Using RP_2, the average time for the VMAT planning was reduced by 88 minutes compared with the clinical plan.

Conclusion: The RapidPlan model with two registered pseudo-structures could generate clinically acceptable plans while saving time.

Key words: knowledge-based planning; RapidPlan; cervical cancer; pseudo-structure

Rep Pract Oncol Radiother 2021;26(6):849-860

Introduction

Volumetric modulated arc therapy (VMAT) with concurrent chemotherapy has been widely used for post-operative patients with uterine cervi-

cal cancer [1]. VMAT can achieve excellent treatment outcomes for cervical cancer while effectively reducing gastrointestinal and urinary toxicity in comparison with three-dimensional conformal radiotherapy [2].

Address for correspondence: Hajime Monzen, Department of Medical Physics, Graduate School of Medical Sciences, Kindai University, 377-2 Ono-higashi, Osakasayama, Osaka 589-8511, Japan, tel: (+81) 72-366-0221, fax: (+81) 72-366-0206; e-mail: hmon@med.kindai.ac.jp

This article is available in open access under Creative Common Attribution-Non-Commercial-No Derivatives 4.0 International (CC BY-NC-ND 4.0) license, allowing to download articles and share them with others as long as they credit the authors and the publisher, but without permission to change them in any way or use them commercially

Recently, there has been interest in adaptive radiotherapy (ART), in which the radiation treatment plan delivered to a patient is modified during the radiotherapy course to account for temporal changes in anatomy due to weight loss, organ motion, and tumor shrinkage [3]. ART is particularly effective in the treatment of cervical cancer, as the large and complex geometrical variations in the pelvic region can limit the potential positive effects of VMAT [4]. However, to generate an adaptive plan requires a replanning process that includes re-contouring and re-optimization, which increases workload and planning time [5].

The RapidPlan treatment planning system (RP; Varian Medical Systems, Palo Alto CA, USA), which performs knowledge-based planning (KBP), can improve both plan consistency and planning efficiency [6]. The RP model is made using structures representing the target volumes and organs at risk (OARs), the dose prescription, and the beam arrangements of previous clinical plans. Many studies have reported that KBP can reduce inter-institutional variations in plan quality, reduce treatment planning times using single optimization, and improve dose sparing of OARs compared with clinical manually-optimized plans [7–19]. The mechanical performance and dosimetric accuracy of RP have also been verified, showing that RP can be safely used in clinical practice [20]. Moreover, it was reported that adaptive plans could be generated with the assistance of RP [21, 22]. However, the original target volumes and OAR structures were registered in most of the RP models used in these studies, and the contouring process part of the replanning still remains labor-intensive and time-consuming.

In practice, the planner generates the contours of virtual structures, so-called “pseudo-structures”, to which the planning dose constraints are imposed [23]. These pseudo-structures can be created very simply and easily using Boolean operations. Castriconi et al. showed the efficiency of plan creation in ART by combining RP and pseudo-structure methods for rectal cancer [24]. They introduced a 2 cm shell pseudo-structure around the PTV with the aim of obtaining a steep dose gradient without losing the dose coverage. However, in their study, the pseudo-structure was not registered in the model, and scaling was performed from the data of twenty plans in order to appropriately weight

the pseudo-structure constraint for optimization. Therefore, there has been no report that evaluates the performance of fully automated optimization by RP with pseudo-structures registered in the model. Moreover, the impact of reducing the number of registered structures in the model on the performance of RP also remains unclear.

Our previous report showed that the performance of RP was influenced by the plan quality registered in the model [25, 26]. Thus, a multi-institutional study with multiple models would be helpful to evaluate the performance of RP. In this study, we retrospectively contoured simple pseudo-structures in cervical cancer patients who were previously treated at each institute. Pseudo-structures were created to improve dose conformity around the PTV and reduce the dose to the OARs. Three patterns of models with different numbers of registered structures were created at each institute, and these models were used to generate treatment plans for new patients not used in the models. The aim of this study was to investigate the performance of RP using a model with registered pseudo-structures, and to determine how many structures are required for automatic optimization of VMAT for postoperative uterine cervical cancer.

Materials and methods

Clinical VMAT plan setting for cervical cancer at each institute registered in the model

This study enrolled five Japanese institutes (A–E). These institutes used VMAT to treat patients with high-risk postoperative uterine cervical cancer. The clinical VMAT plans at each institute were created mainly according to the Japan Clinical Oncology Group (JCOG) 1402 protocol [27, 28]. The clinical target volumes (CTVs) and OARs in the JCOG1402 protocol were contoured according to the CTV contouring guidelines [29] and the Radiation Therapy Oncology Group guidelines for OARs [30]. At each institute, these clinical VMAT plans were created with manual optimization using an unlimited number of pseudo-structures.

Common pseudo-structure contours

We propose the use of pseudo-structures as a more efficient method for the VMAT optimization.

tion and contouring process for the ART phase. In VMAT of postoperative cervical cancer, the target is a single planning target volume (PTV) dose level, which is a relatively simple dose distribution, unlike more complex sites, such as the head and neck region. Therefore, the control region roughly divided into two, the anterior organ and the peripheral organ, and registered in the RP model. For patients who had completed treatment at each institution, three common pseudo-structures were retrospectively contoured, according to the procedure manual:

1. Control_ Anterior (A): Control_A was created from the union of the bowel bag and bladder area, and was cropped from the PTV by 7 mm.
2. Control_ Peripheral (P): Control_P was created by contouring a 2–3 cm cylindrical shell around the PTV and was cropped from the PTV and Control_A by 7 mm.
3. Control_ A P: Control_ A P was created from the union of Control_A and Control_P.

These pseudo-structures were inspired by those used in clinical practice and in the report by Castriconi et al. [24]. In previous reports for VMAT optimization, the distance of the dose gradient region between the PTV and the pseudo-structures was cropped by 5–10 mm [31]. In this study, a dose gradient region of 7 mm was adopted. Details of the contoured pseudo-structures are shown in Figure 1. These pseudo-structures were simply created using Boolean operations and interpolation.

RapidPlan model configuration

The RP algorithm was explained in detail by Fogliata et al. [22]. First, in the model building, the contoured pseudo-structures of the patients were registered. To evaluate the impact of the number of structures registered in the model on the performance of RP, three model patterns with different numbers of registered structures were created at each institute. The process for contouring pseudo-structures and configuring the three model patterns is shown in Figure 2. Model_2, Model_4, and Model_5 had two, four, and five structures registered in the model, respectively. Details of the RP models of each institute are shown in Table 1.

The second step was a training phase based on information extracted from data such as dosimetric and geometric information. These data could be analyzed from the website of Model Analytics (<https://ModelAnalytics.varian.com>). The Model Analytics data also included information about structures or patients that were found to be potential outliers according to numerical metrics, although we did not remove these statistical outliers from the training set used in this study. This is because it has been reported that the impact of removing statistical outliers from the training set was negligible [32, 33].

The third step was selection of the optimization objectives and their priorities. Line, upper, and lower objectives, and priorities, were selected at each institute for each structure in the model, as shown in Table 2. Finally, these models were de-

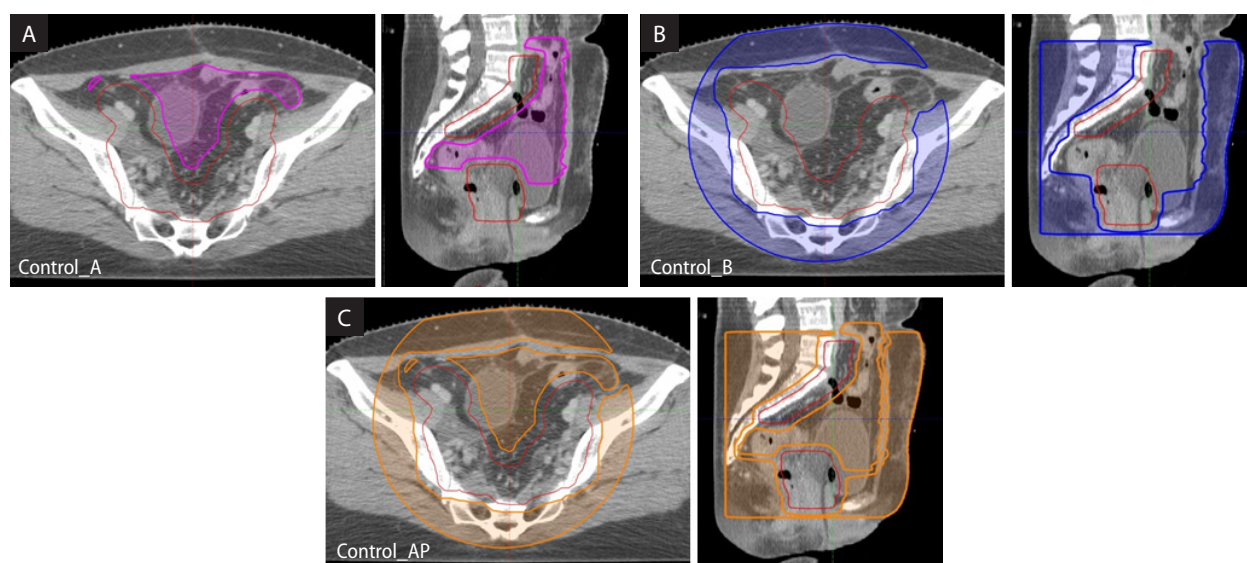


Figure 1. Contouring of Control_A (A), Control_P (B) and Control_A P (C). Red contours represent the planning target volume

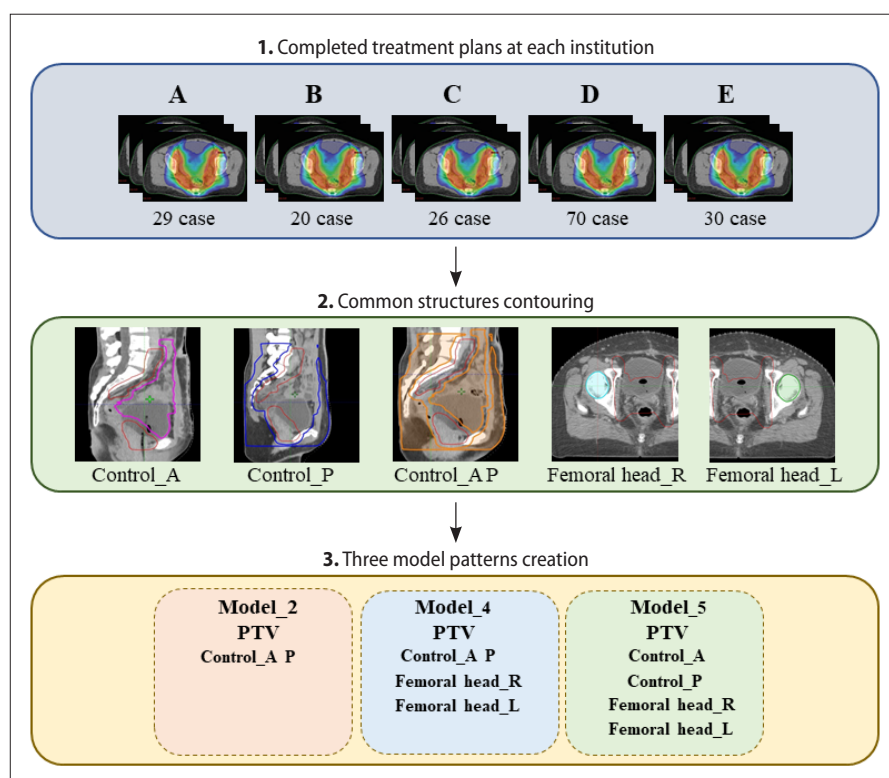


Figure 2. The process of contouring pseudo-structures and configuring the three model patterns. Letters A to E represent the different institutions

Table 1. The RapidPlan model data at each institution

	Model				
	A	B	C	D	E
Number of registered cases	29	20	26	70	30
Mean volume \pm SD [cm ³]					
Mean dose \pm SD (%)					
PTV	1105.9 \pm 99.7 100.5 \pm 0.4	1009.6 \pm 166.3 103.2 \pm 1.3	973.1 \pm 138.0 99.2 \pm 0.2	983.6 \pm 130.8 98.9 \pm 0.2	912.1 \pm 149.6 99.2 \pm 0.1
Control_A	864.4 \pm 237.2 53.1 \pm 3.0	1162.2 \pm 502.9 42.5 \pm 5.3	1299.1 \pm 365.1 45.0 \pm 4.6	1434.5 \pm 441.1 41.8 \pm 4.7	1185.8 \pm 419.1 43.9 \pm 2.9
Control_P	2973.7 \pm 631.5 45.9 \pm 4.2	4217.5 \pm 1258.9 43.0 \pm 3.6	2792.0 \pm 465.2 47.7 \pm 2.5	3235.6 \pm 553.2 41.3 \pm 3.2	2683.4 \pm 344.1 50.8 \pm 2.6
Control_A P	3967.5 \pm 480.5 46.6 \pm 4.1	5380.2 \pm 1708.7 42.9 \pm 3.6	4099.0 \pm 626.3 46.7 \pm 2.4	4696.8 \pm 769.8 41.2 \pm 3.1	3869.8 \pm 527.4 48.7 \pm 2.3
Femoral head_R	38.1 \pm 5.5 50.5 \pm 3.8	44.0 \pm 9.1 54.1 \pm 10.8	48.8 \pm 18.7 44.2 \pm 9.9	36.8 \pm 5.8 45.4 \pm 7.1	43.0 \pm 11.1 47.6 \pm 4.0
Femoral head_L	37.8 \pm 5.0 51.8 \pm 3.7	44.7 \pm 9.9 53.8 \pm 10.7	48.2 \pm 17.5 48.2 \pm 10.1	36.6 \pm 5.7 45.0 \pm 6.1	42.2 \pm 10.9 48.1 \pm 3.5

PTV — planning target volume; Control_A — Control_Anterior; Control_P — Control_Peripheral; Femoral head_R — right femoral head; Femoral head_L — left femoral head

livered to institute A to create treatment plans for common patients. Written informed consent was

obtained from all patients, and the institutional ethics committee approved this study (Japanese Foun-

Table 2. Configuration of the objective for each structure used in RapidPlan

Structures	Institute	Objective	Vol. (%)	Dose	Priority
PTV	A	Upper	0	52.4 Gy	70
		Upper	0.3	52.0 Gy	70
		Lower	100	50.4 Gy	70
		Lower	95	51.4 Gy	70
	B	Upper	0	101 %	Generated
		Lower	100	99 %	Generated
	C	Upper	0	100 %	Generated
		Lower	100	100 %	Generated
	D	Upper	0	100 %	Generated
		Lower	100	100 %	Generated
	E	Upper	0	101 %	100
		Lower	100	100 %	120
Control_A	A	Upper	0	35.0 Gy	Generated
		Upper	Generated	30.0 Gy	Generated
		Line	Generated	Generated	Generated
	B	Line	Generated	Generated	Generated
	C	Line	Generated	Generated	Generated
	D	Line	Generated	Generated	Generated
	E	Line	Generated	Generated	Generated
Control_P	A	Upper	Generated	35.0 Gy	Generated
		Line	Generated	Generated	Generated
	B	Line	Generated	Generated	Generated
	C	Upper	0	100 %	Generated
		Line	Generated	Generated	Generated
	D	Line	Generated	Generated	Generated
	E	Line	Generated	Generated	Generated
Control_A P	A	Upper	0	35.0 Gy	Generated
		Upper	Generated	30.0 Gy	Generated
		Line	Generated	Generated	Generated
	B	Line	Generated	Generated	Generated
	C	Upper	0	100 %	Generated
		Line	Generated	Generated	Generated
	D	Line	Generated	Generated	Generated
	E	Upper	0	45.0 Gy	150
		Upper	50	25.0 Gy	Generated
	Line	Generated	Generated	Generated	
Femoral head_R	A	Upper	Generated	30.0 Gy	Generated
		Line	Generated	Generated	Generated
	B	Line	Generated	Generated	Generated
	C	Line	Generated	Generated	Generated
	D	Line	Generated	Generated	Generated
	E	Line	Generated	Generated	Generated



Table 2. Configuration of the objective for each structure used in RapidPlan

Structures	Institute	Objective	Vol. (%)	Dose	Priority
Femoral head_L	A	Upper	Generated	30.0 Gy	Generated
		Line	Generated	Generated	Generated
	B	Line	Generated	Generated	Generated
	C	Line	Generated	Generated	Generated
	D	Line	Generated	Generated	Generated
	E	Line	Generated	Generated	Generated

PTV — planning target volume; Control_A — Control_Anterior; Control_P — Control_Peripheral; Femoral head_R — right femoral head; Femoral head_L — left femoral head

ation for Cancer Research review board number: 2019-1045).

Evaluation of RapidPlan performance

The RP performance evaluation dataset consisted of the CT data and clinical manually-optimized plans of 22 postoperative uterine cervical cancer patients treated between 2015 and 2019 at institute A. This dataset was independent of that used in the model library. For each patient, a CT-scan was acquired with 2.0-mm slice thickness and a 50-cm field of view. Pseudo-structures were also retrospectively contoured on the CT images.

Without manual intervention and normal tissue objectives, VMAT plans were created at institute A with a single optimization using each RP model and the setting optimization objectives of each institute. For the two-arc VMAT plans with 10-MV photon beams were created using the Photon Optimizer and Anisotropic Analytic Algorithm in the Eclipse treatment planning system Ver 15.6 (Varian Medical Systems, Palo Alto, CA, USA). A dose covering 50% of the PTV of 50.4 Gy in 28 fractions was applied to both the nodal and vaginal cuff PTVs [28]. The plans created by Model_2, Model_4, and Model_5 were identified as RP_2, RP_4, and RP_5, respectively. Comparisons of the treatment plans created by each model were performed using the JCOG1402 dose constraints for PTV and OARs to evaluate the number of structures required for the RP. For the PTV, $D_{98\%}$, $D_{95\%}$, and $D_{2\%}$ were used, whereas D_{max} was used for the overlap between the PTV and bowel bag. For OARs, we used the D_{max} , V_{50Gy} and V_{40Gy} of rectum, D_{max} and V_{45Gy} of bladder, V_{40Gy} of bowel bag, V_{40Gy} and V_{10Gy} of pelvic bones, V_{30Gy} of each femoral head, and D_{max} of the body. Figure 3 shows the process for model transfer and plan comparison.

To evaluate the target coverage, we analyzed the homogeneity index (HI) and conformity index (CI) for the PTV. The HI was calculated as [34]:

$$HI = \frac{D_{2\%} - D_{98\%}}{D_p} \quad (1)$$

Where $D_{2\%}$ = minimum dose to 2% of the target volume indicating the “maximum dose”, $D_{98\%}$ = minimum dose to 98% of the target volume, indicating the “minimum dose”, and D_p = prescribed dose. The ideal value is zero, and increases as homogeneity decreases.

CI was calculated as follows [35],

$$CI = \frac{V_{RI}}{TV} \quad (2)$$

Where V_{RI} is the volume of the reference dose and TV is the target volume. The ideal value is 1.

Planning efficiency

The average planning times of the clinical manually-optimized plans registered in the model (target contouring, OAR contouring, pseudo-structure creation, and optimization times) were recorded at each institute. On the other hand, in the RP plan, since pseudo-structures were retrospectively contoured for patients who had completed treatment, only the average times of pseudo-structure creation and optimization were recorded.

Statistical analysis

Statistical analyses were performed to identify differences in the plans created by each model. The Kruskal-Wallis test was used to compare the three model patterns. When the Kruskal-Wallis test indicated a statistically significant difference, the Steel-Dwass test was used to determine which pair-wise comparisons differed. All statistical analy-

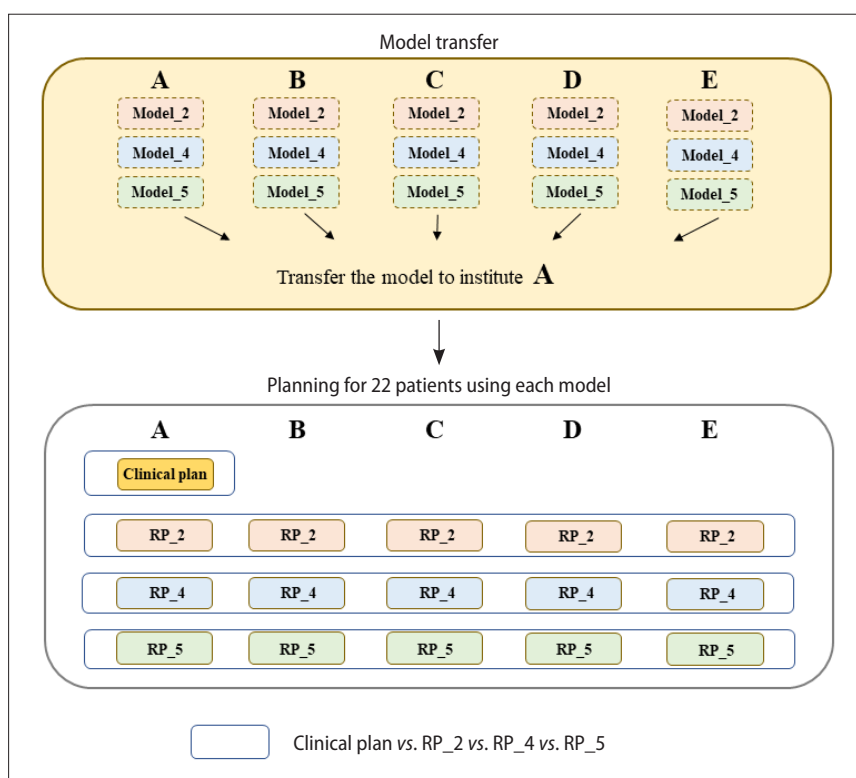


Figure 3. The process for the model transfer and plan comparison. Letters A to E represent the different institutions

ses were conducted with JMP 15.1.0 (SAS Institute, Cary, NC, USA). A value of $p < 0.05$ was considered statistically significant.

Results

Inter-model comparisons

A summary of the dosimetric parameters is listed in Table 3. Box-and-whisker plots of rectum, bowel bag, and femoral head doses for each RP plan at each institute are shown in Figure 4. Most dosimetric parameters showed no major differences across the models, except for the femoral head. The rectum in particular showed no significant differences between the plans created using the respective models at all institutions for all dosimetric parameters. Additionally, the rectum dose of the RP plans was lower than that of the clinical plan.

For the femoral head, there were statistically significant differences between RP_2, RP_4, and RP_5 at all institutes, except institute B. Dose sparing of the femoral heads was worse with RP_2 than with RP_4 and RP_5, but better than that of the clinical plan.

Table 4 shows the proportions of clinical and RP plans achieving the acceptable criteria of the JCOG 1402 protocol. Close to 100% of each of the RP plans achieved the acceptable criteria for most dosimetric parameters. A dose reduction to the femoral head was not achieved with RP_2 in comparison with other models, although performance in terms of the achievement rate was high. For the rectum, although only 74%–85% of the RP plans achieved acceptable V_{40Gy} criteria, the clinical plans achieved similar results.

The PTV HIs (mean \pm 1 SD for all institutions) were 0.10 ± 0.01 , 0.08 ± 0.02 , 0.08 ± 0.02 , and 0.08 ± 0.01 for the clinical plan, RP_2, RP_4, and RP_5, respectively. The PTV CIs (mean \pm 1 SD for all institutions) were 0.51 ± 0.01 , 0.50 ± 0.01 , 0.51 ± 0.01 , and 0.51 ± 0.02 , respectively. Inter-model comparisons of PTV homogeneity and conformity at each institute showed that there were no differences between the models, and that the number of registered structures in the model had no effect on PTV dose. Additionally, in terms of the HI, RP plans performed slightly better than the clinical plan.

Table 3. Summary of the dosimetric parameters in inter-model comparisons

Structures	Average ± SD	Clinical plan	RP_2	RP_4	RP_5	p-value
PTV	D _{98%} (%)	93.3 ± 1.0	94.5 ± 1.8	94.9 ± 1.5	94.5 ± 1.2	0.03
	D _{95%} (%)	95.1 ± 0.8	95.8 ± 1.5	96.2 ± 1.3	96.0 ± 1.0	0.1
	D _{2%} (%)	103.0 ± 0.4	102.7 ± 0.5	102.6 ± 0.4	102.8 ± 0.4	< 0.001
Overlap between PTV and bowel bag	D _{max} (%)	104.5 ± 0.6	105.0 ± 1.0	105.1 ± 1.0	105.4 ± 1.0	< 0.01
Rectum	V _{40Gy} (%)	82.9 ± 13.4	77.9 ± 15.3	80.5 ± 14.9	82.3 ± 15.7	0.06
	V _{50Gy} (%)	33.7 ± 15.9	23.4 ± 10.9	25.4 ± 10.6	25.4 ± 11.3	0.27
	D _{max} (%)	103.8 ± 0.7	102.6 ± 0.9	102.7 ± 1.1	103.0 ± 1.7	0.63
Bladder	V _{45Gy} (%)	34.2 ± 8.3	39.0 ± 10.2	43.2 ± 12.9	36.9 ± 9.5	< 0.001
	D _{max} (%)	103.9 ± 0.8	103.7 ± 1.0	103.7 ± 1.0	104.1 ± 1.1	< 0.001
Bowel bag	V _{40Gy} (%)	32.5 ± 6.6	34.5 ± 8.7	35.8 ± 9.1	31.6 ± 7.5	< 0.01
Pelvic bones	V _{10Gy} (%)	87.3 ± 3.0	87.8 ± 3.2	86.8 ± 3.5	86.9 ± 3.3	0.01
	V _{40Gy} (%)	20.6 ± 3.8	18.5 ± 3.5	18.7 ± 3.3	20.5 ± 4.2	< 0.001
Femoral head_R	V _{30Gy} (%)	18.9 ± 6.4	17.5 ± 11.9	7.4 ± 8.0	8.0 ± 8.9	< 0.001
Femoral head_L	V _{30Gy} (%)	17.3 ± 7.8	16.2 ± 14.8	6.9 ± 6.9	9.2 ± 7.4	< 0.001
Body	D _{max} (%)	106.6 ± 1.1	105.9 ± 1.0	105.9 ± 1.1	106.2 ± 1.2	0.21

PTV — planning target volume; Femoral head_R — right femoral head; Femoral head_L — left femoral head; D_{max} — maximum dose; D_{98%}, D_{95%}, and D_{2%} the dose received by at least 98%, 95% and 2.0% of the volume, V_{50Gy}, V_{45Gy}, V_{40Gy}, V_{30Gy} and V_{10Gy} the OAR volume that receives a dose exceeding 50 Gy, 45 Gy, 40 Gy, 30 Gy and 10 Gy

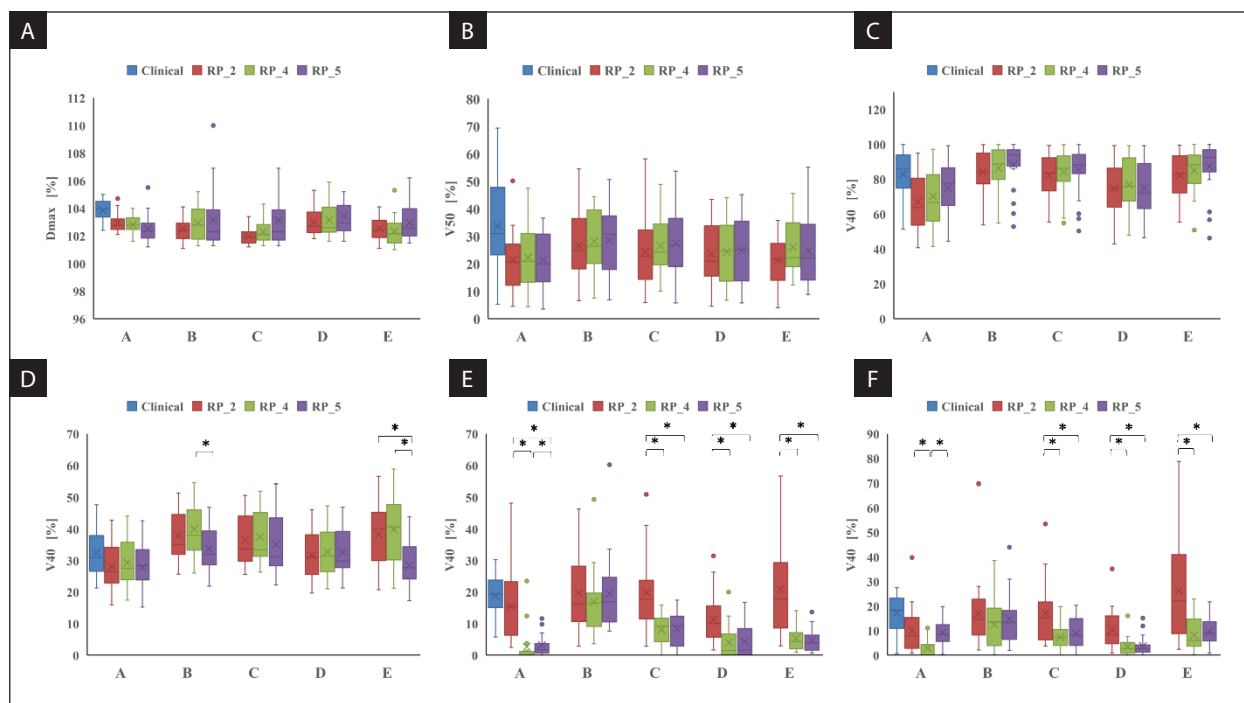


Figure 4. Box-and-whisker plots showing Rectum D_{max} (A), Rectum V_{50Gy} (B), Rectum V_{40Gy} (C), Bowel bag V_{40Gy} (D), Femoral head_R V_{40Gy} (E), Femoral head_L V_{40Gy} (F). The upper and lower edges represent the 25th (Q1) and 75th (Q3) percentiles, respectively. Whiskers represent the standard deviation. Outliers are marked with circles and were defined according to 1.5 × the interquartile range. *p < 0.05. Letters A to E represent the different institutions

Table 4. The proportions of plans achieving acceptable criteria of the JCOG 1402 protocol

Structures		Acceptable objective	Clinical plan	RP_2	RP_4	RP_5
PTV	D _{98%}	> 85%	100%	100%	100%	100%
	D _{95%}	> 90%	100%	100%	100%	100%
	D _{2%}	< 115%	100%	100%	100%	100%
Overlap between PTV and bowel bag	D _{max}	< 110%	100%	100%	100%	100%
Rectum	V _{40Gy}	< 95%	77%	85%	79%	74%
	V _{50Gy}	< 60%	95%	100%	100%	100%
	D _{max}	< 120%	100%	100%	100%	100%
Bladder	V _{45Gy}	< 70%	100%	100%	96%	100%
	D _{max}	< 120%	100%	100%	100%	100%
Bowel bag	V _{40Gy}	< 50%	100%	97%	95%	100%
Pelvic bones	V _{10Gy}	< 95%	100%	100%	100%	100%
	V _{40Gy}	< 50%	100%	100%	100%	100%
Femoral head_R	V _{30Gy}	< 60%	100%	100%	100%	99%
Femoral head_L	V _{30Gy}	< 60%	100%	98%	100%	100%
Body	D _{max}	< 120%	100%	100%	100%	100%

PTV — planning target volume; Femoral head_R — right femoral head; Femoral head_L — left femoral head, D_{max} — maximum dose; D_{98%}, D_{95%} and D_{2%}, the dose received by at least 98%, 95% and 2.0% of the volume, V_{50Gy}, V_{45Gy}, V_{40Gy}, V_{30Gy} and V_{10Gy}, the OAR volume that receives a dose exceeding 50 Gy, 45 Gy, 40 Gy, 30 Gy and 10 Gy

Table 5. Average time spent on various treatment planning processes

Mean time (minutes)		Clinical plan	RP_2	RP_4	RP_5
Contouring	Targets contouring	105	–	–	–
	OARs contouring	99	–	–	–
VMAT Planning	Pseudo-structures creation	15	2	6	14
	Optimization	90	15	15	15
Total time of planning		315	17	21	29

VMAT — volumetric modulated arc therapy, OAR — organs at risk

Planning time analysis

Table 5 shows the average planning times of the clinical manually-optimized plan and RP plans at each institute, with this time being spent on the various processes of the treatment planning. Using RP_2, RP_4, and RP_5, the average time for the VMAT planning time was reduced by 88, 84, and 76 minutes, respectively, compared with the clinical plan.

Discussion

This multi-institutional study investigated the performance of RP using models with pseudo-structures and determined the optimal number of structures for RP models. Inter-model comparisons showed no major differences for most dosi-

metric parameters, as shown in Table 3 and Fig. 4. Furthermore, Table 4 indicates that most RP plans were able to achieve the acceptable criteria of the JCOG 1402 protocol. Previous publications evaluating RP models showed that KBP plans exceeded the clinical accepted plan quality at various anatomical sites [7, 22, 32]. Although the models in these studies were registered with multiple original OAR structures, the RP performance of our models with only 2–5 structures registered was found to be similar to that reported in previous publications. Moreover, Hussein et al. reported the performance of RP using models with original target volumes and OAR structures for cervical cancer [32], and the dosimetric parameters of their RP plans were comparable to this modeling approach using pseudo-structures. Thus, our results show that training

RP models with pseudo-structures is a simple and effective approach for creating high quality VMAT plans with RP.

The dosimetric parameter results in Table 3 and Fig. 4, and the proportions of plans achieving acceptable criteria in Table 4, indicating that Model_2 using only the PTV and Control_A P showed good dosimetric performance at all institutes. As shown in Table 2, a line objective was commonly used for Control_A P at each institute. The good dosimetric performance of Model_2 is helped by the use of the line objective defined slightly below the estimated dose volume histogram (DVH) lower bound, which helps to drive the optimization towards the best estimated DVH [36]. As the weights for the points on each line objective are all equal, reducing the average dose for large volume structures may be more effective. However, the dose sparing of the femoral head in RP_2 was the worst among the RP models at each institute. This was because the Control_A P pseudo-structure did not impose dose constraints locally on the femoral head. However, the proportions of plans achieving acceptable criteria in the right and left femoral heads were 100% and 98%, respectively. Model_5, in which Control_A P was divided and registered in the model, also showed no dose-reduction advantage in the rectum, bladder, and pelvic bone in comparison with Model_2. Fogliata et al. also reported that there were no significant differences in the plans generated using two models with different management of the parotid gland (ipsi- and contra-lateral parotids in the model vs. integration into one structure) and that the dose differences were very small [37]. Therefore, we conclude that the RP model can perform adequately with the registration of two structures.

Compared with the clinical plans, the RP plans showed better dose coverage and OAR sparing. In particular, the RP plans reduced the rectum dose. In JCOG1402, posterior margin of the CTV vaginal cuff is the anterior part of the mesorectal fascia or anterior wall of the rectum, thus including the rectum within the PTV margin [28]. Therefore, the clinical plan could not impose strong constraints for the rectum in order to obtain a sufficient target dose. On the other hand, in the RP plans, a steep dose gradient was obtained due to the pseudo-structure around the PTV, and the rectum doses were reduced. By registering the pseudo-structures

in the RP model, appropriate constraints were automatically imposed on the OARs around the PTV.

The potential benefit of this modeling approach using pseudo-structures is time efficiency. In practice, the correcting of tumor and normal tissue variations through modification of the original plan is hampered by the time-consuming re-planning process, which currently represents the major obstacle for large scale implementation of this strategy [38]. Recently, the use of deformable image registration (DIR) for automatic propagation of structures in ART has been widely investigated. However, registration errors may still exist with DIR, especially for structures that are small and lack contrast with the background, and these registration errors could result in significant dosimetric deviation [39]. Additionally, Nelson et al. reported a total planning time of 207.5 minutes for OAR contouring and optimization, when implementing DIR in an adaptive plan with the assistance of KBP [21]. Acharya et al. reported that the median time for even online ART using an MR Linac was 26 minutes, including re-contouring, re-optimization, and patient-specific quality assurance [40]. As Table 5 shows, the plan created using Model_2 took only 17 minutes for the pseudo-structure creation and optimization process. Therefore, this modeling approach using pseudo-structures should be useful for ART strategies.

The KBP approach has the advantage that its model can be shared by multiple institutions. Sharing of models is considered to be a good method for reducing variability in planning quality across multiple institutions [25]. In the present study, we were able to create a plan achieving acceptable criteria with a model that was created using only a simple procedure manual. Therefore, the model can be easily shared by creating pseudo-structures at each institute. It was also reported that inter-observer contouring variations have a significant impact on dosimetric and radiobiological outcomes in intensity modulated radiation therapy planning [41]. Reducing the number of structures is useful as a means of homogenizing treatment plan quality across institutions.

The planning quality evaluation in this study was conducted only for cervical cancer patients, and there is a limitation in that the methods in this study cannot cover treatment plans for several PTV dose levels using a simultaneous integrated boost

(SIB), such as is performed in head and neck cancer patients; management of the dose gradient around PTVs is more complex with SIB-VMAT plans. In addition, the structures used for the dose evaluation were not considered in this study, but may be defined using automatic segmentation methods.

Conclusions

The RP_2 achieved clinically-acceptable criteria, and comparable dosimetric parameters to the clinical plan, RP_4, and RP_5. The RP model with two registered pseudo-structures could generate a clinically-acceptable plan while saving considerable time. The RP modeling approach was simple and might be useful for ART strategies.

Acknowledgements

We thank Karl Embleton, PhD, from Edanz Group (<https://en-author-services.edanzgroup.com/>) for editing a draft of this manuscript.

Conflict of interest

The authors declare that they have no competing interests.

Funding

This study was supported by a JSPS KAKENHI Grant [grant number 17 K15817] and Japanese Society of Radiological Technology (JSRT) Research Grant (2019, 2020).

References

1. Yuan Y, You J, Wang W, et al. Long-term follow-up of volumetric modulated arc therapy in definitive radiotherapy for cervical cancer: A single-center retrospective experience. *Radiat Med Protect*. 2020; 1(2): 81–87, doi: [10.1016/j.radmp.2020.04.002](https://doi.org/10.1016/j.radmp.2020.04.002).
2. Lin Y, Ouyang Y, Chen K, et al. Long-term follow-up of volumetric modulated arc therapy in definitive radiotherapy for cervical cancer: A single-center retrospective experience. *Front Oncol*. 2019; 9: 760.
3. Tan LT, Tanderup K, Kirisits C, et al. Image-guided Adaptive Radiotherapy in Cervical Cancer. *Semin Radiat Oncol*. 2019; 29: 284–98, doi: [10.1016/j.semradonc.2019.02.010](https://doi.org/10.1016/j.semradonc.2019.02.010).
4. Heijkoop S.T. Plan-of-the-day Adaptive Radiotherapy for Locally Advanced Cervical Cancer. Erasmus University Rotterdam, 2017. <http://hdl.handle.net/1765/102419> (12 July 2020).
5. Dial C, Weiss E, Siebers JV, et al. Benefits of adaptive radiation therapy in lung cancer as a function of replanning frequency. *Med Phys*. 2016; 43(4): 1787, doi: [10.1118/1.4943564](https://doi.org/10.1118/1.4943564), indexed in Pubmed: [27036576](https://pubmed.ncbi.nlm.nih.gov/27036576/).
6. Fusella M, Scaggion A, Pivato N, et al. Efficiently train and validate a RapidPlan model through APQM scoring. *Med Phys*. 2018; 45(6): 2611–2619, doi: [10.1002/mp.12896](https://doi.org/10.1002/mp.12896), indexed in Pubmed: [29611213](https://pubmed.ncbi.nlm.nih.gov/29611213/).
7. Tol JP, Delaney AR, Dahele M, et al. Evaluation of a knowledge-based planning solution for head and neck cancer. *Int J Radiat Oncol Biol Phys*. 2015; 91(3): 612–620, doi: [10.1016/j.ijrobp.2014.11.014](https://doi.org/10.1016/j.ijrobp.2014.11.014), indexed in Pubmed: [25680603](https://pubmed.ncbi.nlm.nih.gov/25680603/).
8. Fogliata A, Nicolini G, Clivio A, et al. A broad scope knowledge based model for optimization of VMAT in esophageal cancer: validation and assessment of plan quality among different treatment centers. *Radiat Oncol*. 2015; 10: 220, doi: [10.1186/s13014-015-0530-5](https://doi.org/10.1186/s13014-015-0530-5), indexed in Pubmed: [26521015](https://pubmed.ncbi.nlm.nih.gov/26521015/).
9. Wu H, Jiang F, Yue H, et al. A dosimetric evaluation of knowledge-based VMAT planning with simultaneous integrated boosting for rectal cancer patients. *J Appl Clin Med Phys*. 2016; 17(6): 78–85, doi: [10.1120/jacmp.v17i6.6410](https://doi.org/10.1120/jacmp.v17i6.6410), indexed in Pubmed: [27929483](https://pubmed.ncbi.nlm.nih.gov/27929483/).
10. Kubo K, Monzen H, Ishii K, et al. Dosimetric comparison of RapidPlan and manually optimized plans in volumetric modulated arc therapy for prostate cancer. *Phys Med*. 2017; 44: 199–204, doi: [10.1016/j.ejmp.2017.06.026](https://doi.org/10.1016/j.ejmp.2017.06.026), indexed in Pubmed: [28705507](https://pubmed.ncbi.nlm.nih.gov/28705507/).
11. Kubo K, Monzen H, Ishii K, et al. Inter-planner variation in treatment-plan quality of plans created with a knowledge-based treatment planning system. *Phys Med*. 2019; 67: 132–140, doi: [10.1016/j.ejmp.2019.10.032](https://doi.org/10.1016/j.ejmp.2019.10.032), indexed in Pubmed: [31706149](https://pubmed.ncbi.nlm.nih.gov/31706149/).
12. Ueda Y, Miyazaki M, Sumida I, et al. Knowledge-based planning for oesophageal cancers using a model trained with plans from a different treatment planning system. *Acta Oncol*. 2020; 59(3): 274–283, doi: [10.1080/0284186X.2019.1691257](https://doi.org/10.1080/0284186X.2019.1691257), indexed in Pubmed: [31755332](https://pubmed.ncbi.nlm.nih.gov/31755332/).
13. Uehara T, Monzen H, Tamura M, et al. Dose-volume histogram analysis and clinical evaluation of knowledge-based plans with manual objective constraints for pharyngeal cancer. *J Radiat Res*. 2020; 61(3): 499–505, doi: [10.1093/jrr/rraa021](https://doi.org/10.1093/jrr/rraa021), indexed in Pubmed: [32329509](https://pubmed.ncbi.nlm.nih.gov/32329509/).
14. Inoue E, Doi H, Monzen H, et al. Dose-volume Histogram Analysis of Knowledge-based Volumetric-modulated Arc Therapy Planning in Postoperative Breast Cancer Irradiation. *In Vivo*. 2020; 34(3): 1095–1101, doi: [10.21873/invivo.11880](https://doi.org/10.21873/invivo.11880), indexed in Pubmed: [32354897](https://pubmed.ncbi.nlm.nih.gov/32354897/).
15. Tamura M, Monzen H, Matsumoto K, et al. Influence of Cleaned-up Commercial Knowledge-Based Treatment Planning on Volumetric-Modulated Arc Therapy of Prostate Cancer. *J Med Phys*. 2020; 45(2): 71–77, doi: [10.4103/jmp.JMP_109_19](https://doi.org/10.4103/jmp.JMP_109_19), indexed in Pubmed: [32831489](https://pubmed.ncbi.nlm.nih.gov/32831489/).
16. Monzen H, Tamura M, Ueda Y, et al. Dosimetric evaluation with knowledge-based planning created at different periods in volumetric-modulated arc therapy for prostate cancer: a multi-institution study. *Radiol Phys Technol*. 2020; 13(4): 327–335, doi: [10.1007/s12194-020-00585-0](https://doi.org/10.1007/s12194-020-00585-0), indexed in Pubmed: [32986184](https://pubmed.ncbi.nlm.nih.gov/32986184/).
17. Ueda Y, Monzen H, Fukunaga JI, et al. Characterization of knowledge-based volumetric modulated arc therapy plans created by three different institutions' models for prostate cancer. *Rep Pract Oncol Radiother*. 2020; 25(6): 1023–1028, doi: [10.1016/j.rpor.2020.08.011](https://doi.org/10.1016/j.rpor.2020.08.011), indexed in Pubmed: [33390859](https://pubmed.ncbi.nlm.nih.gov/33390859/).

18. Ito T, Tamura M, Monzen H, et al. [Impact of Aperture Shape Controller on Knowledge-based VMAT Planning of Prostate Cancer]. *Nihon Hoshasen Gijutsu Gakkai Zasshi*. 2021; 77(1): 23–31, doi: [10.6009/jjrt.2021_JSRT_77.1.23](https://doi.org/10.6009/jjrt.2021_JSRT_77.1.23), indexed in Pubmed: [33473076](https://pubmed.ncbi.nlm.nih.gov/33473076/).
19. Wada Y, Monzen H, Tamura M, et al. Dosimetric Evaluation of Simplified Knowledge-Based Plan with an Extensive Stepping Validation Approach in Volumetric-Modulated Arc Therapy-Stereotactic Body Radiotherapy for Lung Cancer. *J Med Phys*. 2021; 46(1): 7–15, doi: [10.4103/jmp.JMP_67_20](https://doi.org/10.4103/jmp.JMP_67_20), indexed in Pubmed: [34267484](https://pubmed.ncbi.nlm.nih.gov/34267484/).
20. Tamura M, Monzen H, Matsumoto K, et al. Mechanical performance of a commercial knowledge-based VMAT planning for prostate cancer. *Radiat Oncol*. 2018; 13(1): 163, doi: [10.1186/s13014-018-1114-y](https://doi.org/10.1186/s13014-018-1114-y), indexed in Pubmed: [30170614](https://pubmed.ncbi.nlm.nih.gov/30170614/).
21. Fung NT, Hung WM, Sze CK, et al. Automatic segmentation for adaptive planning in nasopharyngeal carcinoma IMRT: Time, geometrical, and dosimetric analysis. *Med Dosim*. 2020; 45(1): 60–65, doi: [10.1016/j.meddos.2019.06.002](https://doi.org/10.1016/j.meddos.2019.06.002), indexed in Pubmed: [31345672](https://pubmed.ncbi.nlm.nih.gov/31345672/).
22. Fogliata A, Wang PM, Belosi F, et al. Assessment of a model based optimization engine for volumetric modulated arc therapy for patients with advanced hepatocellular cancer. *Radiat Oncol*. 2014; 9: 236, doi: [10.1186/s13014-014-0236-0](https://doi.org/10.1186/s13014-014-0236-0), indexed in Pubmed: [25348465](https://pubmed.ncbi.nlm.nih.gov/25348465/).
23. Neve WD, Wu Y, Ezzell G. *Practical IMRT Planning. Image-guided IMRT*. Springer, Berlin 2006: 49–54.
24. Castriconi R, Fiorino C, Passoni P, et al. Knowledge-based automatic optimization of adaptive early-regression-guided VMAT for rectal cancer. *Phys Med*. 2020; 70: 58–64, doi: [10.1016/j.ejmp.2020.01.016](https://doi.org/10.1016/j.ejmp.2020.01.016), indexed in Pubmed: [31982788](https://pubmed.ncbi.nlm.nih.gov/31982788/).
25. Ueda Y, Fukunaga JI, Kamima T, et al. Evaluation of multiple institutions' models for knowledge-based planning of volumetric modulated arc therapy (VMAT) for prostate cancer. *Radiat Oncol*. 2018; 13(1): 46, doi: [10.1186/s13014-018-0994-1](https://doi.org/10.1186/s13014-018-0994-1), indexed in Pubmed: [29558940](https://pubmed.ncbi.nlm.nih.gov/29558940/).
26. Kamima T, Ueda Y, Fukunaga JI, et al. Multi-institutional evaluation of knowledge-based planning performance of volumetric modulated arc therapy (VMAT) for head and neck cancer. *Phys Med*. 2019; 64: 174–181, doi: [10.1016/j.ejmp.2019.07.004](https://doi.org/10.1016/j.ejmp.2019.07.004), indexed in Pubmed: [31515017](https://pubmed.ncbi.nlm.nih.gov/31515017/).
27. Murakami N, Isohashi F, Hasumi Y, et al. Single-arm confirmatory trial of postoperative concurrent chemoradiotherapy using intensity modulated radiation therapy for patients with high-risk uterine cervical cancer: Japan Clinical Oncology Group study (JCOG1402). *Jpn J Clin Oncol*. 2019; 49(9): 881–885, doi: [10.1093/jjco/hyz098](https://doi.org/10.1093/jjco/hyz098), indexed in Pubmed: [31613355](https://pubmed.ncbi.nlm.nih.gov/31613355/).
28. Okamoto H, Murakami N, Isohashi F, et al. Dummy-run for standardizing plan quality of intensity-modulated radiotherapy for postoperative uterine cervical cancer: Japan Clinical Oncology Group study (JCOG1402). *Radiat Oncol*. 2019; 14(1): 133, doi: [10.1186/s13014-019-1340-y](https://doi.org/10.1186/s13014-019-1340-y), indexed in Pubmed: [31358026](https://pubmed.ncbi.nlm.nih.gov/31358026/).
29. Toita T, Ohno T, Kaneyasu Y, et al. Japan Clinical Oncology Group. A consensus-based guideline defining the clinical target volume for pelvic lymph nodes in external beam radiotherapy for uterine cervical cancer. *Jpn J Clin Oncol*. 2010; 40(5): 456–463, doi: [10.1093/jjco/hyp191](https://doi.org/10.1093/jjco/hyp191), indexed in Pubmed: [20133334](https://pubmed.ncbi.nlm.nih.gov/20133334/).
30. Gay HA, Barthold HJ, O'Meara E, et al. Pelvic normal tissue contouring guidelines for radiation therapy: a Radiation Therapy Oncology Group consensus panel atlas. *Int J Radiat Oncol Biol Phys*. 2012; 83(3): e353–e362, doi: [10.1016/j.ijrobp.2012.01.023](https://doi.org/10.1016/j.ijrobp.2012.01.023), indexed in Pubmed: [22483697](https://pubmed.ncbi.nlm.nih.gov/22483697/).
31. Chen J, Chen C, Atwood T, et al. Volumetric modulated arc therapy planning method for supine craniospinal irradiation. *J Radiat Oncol*. 2012; 1(3): 291–297, doi: [10.1007/s13566-012-0028-9](https://doi.org/10.1007/s13566-012-0028-9).
32. Hussein M, South CP, Barry MA, et al. Clinical validation and benchmarking of knowledge-based IMRT and VMAT treatment planning in pelvic anatomy. *Radiother Oncol*. 2016; 120(3): 473–479, doi: [10.1016/j.radonc.2016.06.022](https://doi.org/10.1016/j.radonc.2016.06.022), indexed in Pubmed: [27427380](https://pubmed.ncbi.nlm.nih.gov/27427380/).
33. Delaney AR, Tol JP, Dahele M, et al. Effect of Dosimetric Outliers on the Performance of a Commercial Knowledge-Based Planning Solution. *Int J Radiat Oncol Biol Phys*. 2016; 94(3): 469–477, doi: [10.1016/j.ijrobp.2015.11.011](https://doi.org/10.1016/j.ijrobp.2015.11.011), indexed in Pubmed: [26867876](https://pubmed.ncbi.nlm.nih.gov/26867876/).
34. Kataria T, Sharma K, Subramani V, et al. Homogeneity Index: An objective tool for assessment of conformal radiation treatments. *J Med Phys*. 2012; 37(4): 207–213, doi: [10.4103/0971-6203.103606](https://doi.org/10.4103/0971-6203.103606), indexed in Pubmed: [23293452](https://pubmed.ncbi.nlm.nih.gov/23293452/).
35. Feuvret L, Noël G, Mazon JJ, et al. Conformity index: a review. *Int J Radiat Oncol Biol Phys*. 2006; 64(2): 333–342, doi: [10.1016/j.ijrobp.2005.09.028](https://doi.org/10.1016/j.ijrobp.2005.09.028), indexed in Pubmed: [16414369](https://pubmed.ncbi.nlm.nih.gov/16414369/).
36. Fogliata A, Cozzi L, Reggiori G, et al. RapidPlan knowledge based planning: iterative learning process and model ability to steer planning strategies. *Radiat Oncol*. 2019; 14(1): 187, doi: [10.1186/s13014-019-1403-0](https://doi.org/10.1186/s13014-019-1403-0), indexed in Pubmed: [31666094](https://pubmed.ncbi.nlm.nih.gov/31666094/).
37. Fogliata A, Reggiori G, Stravato A, et al. RapidPlan head and neck model: the objectives and possible clinical benefit. *Radiat Oncol*. 2017; 12(1): 73, doi: [10.1186/s13014-017-0808-x](https://doi.org/10.1186/s13014-017-0808-x), indexed in Pubmed: [28449704](https://pubmed.ncbi.nlm.nih.gov/28449704/).
38. Cilla S, Ianiro A, Romano C, et al. Template-based automation of treatment planning in advanced radiotherapy: a comprehensive dosimetric and clinical evaluation. *Sci Rep*. 2020; 10(1): 423, doi: [10.1038/s41598-019-56966-y](https://doi.org/10.1038/s41598-019-56966-y), indexed in Pubmed: [31949178](https://pubmed.ncbi.nlm.nih.gov/31949178/).
39. Li J, Xu Z, Pilar A, et al. Adaptive radiotherapy for nasopharyngeal carcinoma. *Annals of Nasopharynx Cancer*. 2020; 4: 1–1, doi: [10.21037/anpc.2020.03.01](https://doi.org/10.21037/anpc.2020.03.01).
40. Acharya S, Fischer-Valuck BW, Kashani R, et al. Online Magnetic Resonance Image Guided Adaptive Radiation Therapy: First Clinical Applications. *Int J Radiat Oncol Biol Phys*. 2016; 94(2): 394–403, doi: [10.1016/j.ijrobp.2015.10.015](https://doi.org/10.1016/j.ijrobp.2015.10.015), indexed in Pubmed: [26678659](https://pubmed.ncbi.nlm.nih.gov/26678659/).
41. Bhardwaj A, Kehwar TS, Chakarvarti SK, et al. Variations in inter-observer contouring and its impact on dosimetric and radiobiological parameters for intensity-modulated radiotherapy planning in treatment of localised prostate cancer. *J Radiother Pract*. 2008; 7(2): 77–88, doi: [10.1017/s1460396908006316](https://doi.org/10.1017/s1460396908006316).